JOURNAL OF NATURAL PRODUCTS

Article

Cite This: J. Nat. Prod. XXXX, XXX, XXX−XXX

pubs.acs.org/jnp

Linfuranones B and C, Furanone-Containing Polyketides from a Plant-Associated *Sphaerimonospora mesophila*

Hirofumi Akiyama,[†] Chantra Indananda,[‡] Arinthip Thamchaipenet,[§] Atsuko Motojima,[⊥] Tsutomu Oikawa,[⊥] Hisayuki Komaki,[∥] Akira Hosoyama,[#] Akane Kimura,[#] Naoya Oku,[†] and Yasuhiro Igarashi*[,†]

[†]Biotechnology Research Center, Toyama Prefectural University, Imizu, Toyama 939-0398, Japan

[‡]Department of Biology, Faculty of Science, Burapha University, Chonburi 20131, Thailand

[§]Actinobacteria Research Unit, Department of Genetics, Faculty of Science, Kasetsart University, Bangkok 10900, Thailand

[⊥]Department of Nutritional Biochemistry, School of Nutrition and Dietetics, Kanagawa University of Human Services, Yokosuka, Kanagawa 238-8522, Japan

[∥]Biological Resource Center, National Institute of Technology and Evaluation (NBRC), Kisarazu, Chiba 292-0818, Japan

[#]NBRC, Shibuya, Tokyo 151-0066, Japan

Supporting Information

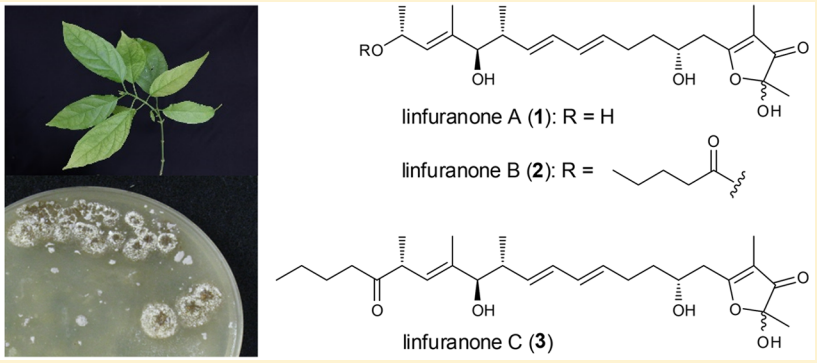

ABSTRACT: Two new furanone-containing polyketides, linfuranones B and C, were isolated from a plant-associated actinomycete of the genus *Sphaerimonospora*. Their structures were determined by NMR and MS spectroscopic analyses, and the absolute configurations were established by anisotropic methods and chemical degradation approaches. *In silico* analysis of biosynthetic genes suggested that linfuranone B is generated from linfuranone C by oxidative cleavage of the polyketide chain. Linfuranones B and C induced preadipocyte differentiation into matured adipocytes at 20−40 μM without showing cytotoxicity.

Bacterial polyketides synthesized by modular polyketide synthases (type I PKSs) are one of the largest groups of natural products. This group is characterized by its structural variation and complexity arising from multiple chiral centers, postmodification by tailoring enzymes, and/or coupling with other pathways such as nonribosomal peptide synthesis.[1] 3(2*H*)-Furanone is a relatively minor structural element in polyketides. To date, ca. 20 linear polyketides bearing a furanone ring at their carboxy terminus have been found from mollusks, fungi, actinomycetes, and myxobacteria (Figure 1).[2]

The actinomycete strain *Sphaerimonospora mesophila* GMKU 363 was isolated from a root tissue of the Thai medicinal herb "Lin Ngu Hoa" (*Clinacanthus siamensis* Bremek.) collected in Chachoengsao Province, Thailand. We previously reported the isolation of a furanone-containing polyketide, linfuranone A (**1**),[3] and then found its acylated congener linfuranone B (**2**), which will be reported in this paper. Accordingly, the draft genome of strain GMKU 363 was sequenced to assess its biosynthetic potential in secondary metabolism as well as to identify the biosynthetic genes for **1** and **2**.[4] A deduced biosynthetic gene cluster contains five PKS genes in which a total of 11 modules are present along with the genes of tailoring enzymes for furanone construction (Figure 11, Table 2).[4] The PKS module organization predicted that the intact PKS product is assembled from six methylmalonates and five malonates (Figure 2). However, contrary to this prediction, the main carbon chain of **1** and **2** is five carbons shorter than that of the predicted structure. This inconsistency between the predicted structure and the actually isolated structures was suggestive of the presence of linfuranone congeners other than **1** and **2**, prompting us to reinvestigate the metabolites of this strain.

Received: January 22, 2018

DOI: 10.1021/acs.jnatprod.8b00071
J. Nat. Prod. XXXX, XXX, XXX−XXX

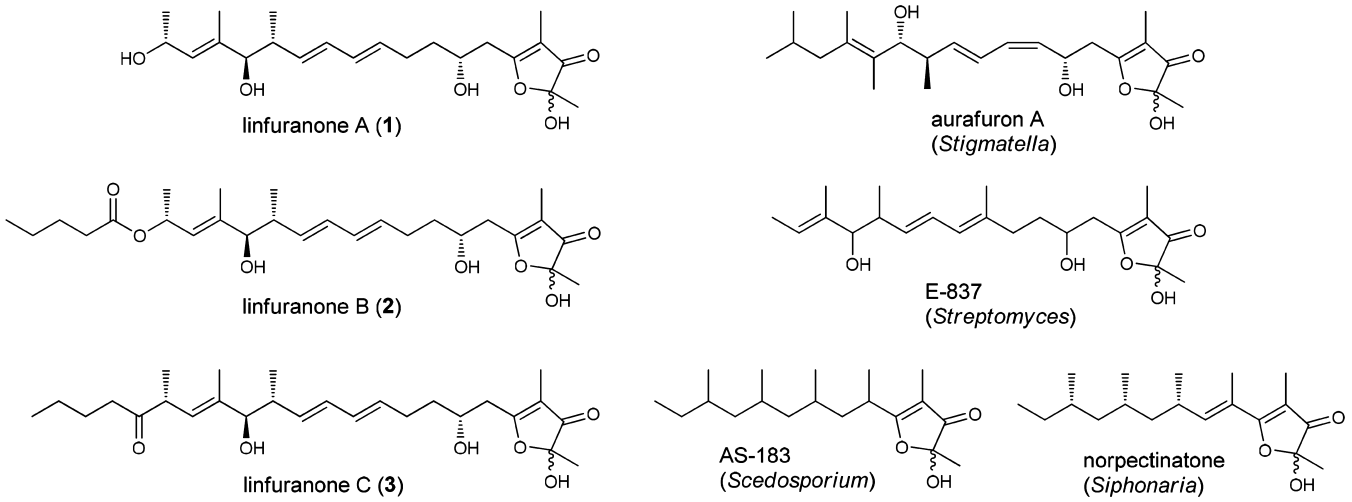

Figure 1. Structures of linfuranones A–C (**1**–**3**) and related 3(2*H*)-furanones.

RESULTS AND DISCUSSION

To search for a metabolite that has the aforementioned predicted skeleton, culture conditions were examined and the optimal growth temperature of strain GMKU 363 was found to be around 37 to 40 °C, higher than the temperature commonly used for secondary metabolite production by actinomycetes as well as for the production of linfuranone A (**1**). The strain was thus precultured and cultured at 37 °C for 4 days and 7 days, respectively, and metabolites were analyzed in comparison with those produced at 30 °C. In the culture extract obtained by fermentation at 37 °C, a new intense peak that showed a similar UV–vis spectrum to the furanone chromophore was observed near the peak of linfuranone B (**2**) (Supporting Information, Figure S17). This new peak was not detectable when the strain was cultured at 30 °C. UV-guided purification from the extract led to the isolation of another furanone-type polyketide, linfuranone C (**3**), that has the same carbon skeleton as the predicted structure (Figures 1 and 2). Herein, we describe the isolation, structure elucidation, biological property, and biosynthesis of **2** and **3**.

Linfuranone B (**2**) was obtained as a pale yellow, amorphous solid. The high-resolution ESITOFMS analysis gave a molecular formula of $C_{27}H_{42}O_7$, which was consistent with the ^{1}H and ^{13}C NMR data. The IR spectrum indicated the presence of hydroxy (3383 cm^{-1}) and carbonyl (1695 and 1611 cm^{-1}) groups. The UV spectrum with the absorption maxima at 232 and 282 nm was closely similar to that of linfuranone A,[3] suggesting that **2** was a new congener. The ^{13}C NMR and HSQC analysis confirmed the presence of 27 carbons attributable to three oxygenated sp^2 carbons, seven olefinic carbons (five are proton-bearing), one hemiketal carbon, four sp^3 methines (three are oxygenated), six sp^3 methylenes, and six methyl carbons. Due to the epimerization at the hemiketal carbon, two separated resonances were observed for some of the protons and carbons (Table 1).[2g−j]

Analysis of the COSY spectrum allowed assignment of five proton spin systems. First, contiguous correlations from H23 to H20, together with HMBC correlations from H20 and H21 to the carbonyl carbon C19 (δ_C 173.7), established an *n*-pentanoyl group. The H18 methine had an HMBC correlation to C19, and thereby the pentanoyl group was connected to C18 through an ester linkage. A five-carbon fragment from H12 to H15 with a methyl substituent on C14 was identified also from the COSY analysis. This fragment was connected to C17 through C16 based on the HMBC correlations from H26 to C15, C16, and C17. Furthermore, the linear carbon chain from C6 to C12, consisting of two fragments H6/H7/H8 and H9/H10/H11, was established by the long-range correlations from H11 to C12, H13 to C11, and H9 and H10 to C6. The presence of a furanone substructure was deduced by the HMBC correlations from the H24 methyl to the three sp^2 carbons C3, C4, and C5 and the H1 methyl to C3 and hemiketal carbon C2. The furanone moiety and the above-defined chain structure were joined at C5 and C6 on the basis of correlations from H6 to C4 and C5. The planar structure of **2** was thus determined as an *O*-acyl congener of **1** (Figure 3).

Absolute configurations at C7 and C15 of **2** were determined by applying the modified Mosher's method.[5] MTPA esterification of **2** by the treatment with (*S*)- or (*R*)-MTPACl gave tris(*R*)- and (*S*)-MTPA esters (**4a** and **4b**). Positive $\Delta\delta_{S-R}$ values for H8 to H14 and H25 protons and negative values for H6, H17, H18, H26, and H27 protons indicated the 7*R* and 15*R* configurations (Figure 4). The relative configuration at C14 was determined on the basis of $^3J_{HH}$ values and NOESY correlations. The large coupling constant of 8.5 Hz between H14 and H15 indicated the *anti* relationship of these protons around the C14–C15 axis (Figure 5). C13 and C16 were also placed in an *anti* position around the same axis on the basis of the NOESY correlations for H13/H15, H14/H26, and H17/H25 (Figure 5). Therefore, the relative configuration of the C25 methyl to 15-OH was assigned *anti*, and thus the 14*R* configuration was established. The remaining C18 configuration was determined by chiral HPLC analysis of a lactic acid fragment obtained by degradation of **2**. Compound **2** was subjected to ozonolysis followed by an oxidative workup with hydrogen peroxide. The reaction mixture was then hydrolyzed in alkaline solution, affording a mixture containing lactic acid derived from three carbons, C17/C18/C19 (Figure 6). Chiral HPLC analysis in comparison with the authentic (*R*)- and (*S*)-lactic acids showed the occurrence of the (*R*)-enantiomer in the degraded product mixture, thereby establishing the 18*R* configuration (Figure 6).

Linfuranone C (**3**) was also obtained as a pale yellow, amorphous solid. Its NMR, IR, and UV spectroscopic data were similar to those for linfuranone B (**2**). The high-

DOI: 10.1021/acs.jnatprod.8b00071
J. Nat. Prod. XXXX, XXX, XXX–XXX

Table 1. ^{1}H and ^{13}C NMR Data for Linfuranones B (2) and C (3) in $CDCl_3$

	linfuranone B (2)			linfuranone C (3)		
position	δ_C	δ_H mult (J in Hz)[a]	HMBC[c]	δ_C[b]	δ_H mult (J in Hz)[a]	HMBC[c]
1	21.8	1.47, s	2, 3	21.9	1.50, s	2, 3
	22.0	1.49, s	2, 3	22.2	1.52, s	2, 3
2	102.8			102.60		
	102.9			102.65		
3	203.3			202.8		
	203.9			203.4		
4	109.3			109.4		
	110.1			110.0		
5	184.9			184.4		
6	37.1	2.55, dd (14.1, 8.0)	4, 5, 7, 8	37.1	2.60, dd (14.3, 8.1)	4, 5, 7, 8
		2.75, m	4, 5, 7, 8		2.74, dd (14.3, 4.2)	4, 5, 7, 8
	37.4	2.46, dd (14.2, 2.8)	4, 5, 7, 8	37.4	2.49, m	4, 5, 7, 8
		2.76, dd (14.2, 5.4)	4, 5, 7, 8		2.75, dd (14.3, 9.5)	4, 5, 7, 8
7	68.4	4.09 m	5	68.9	4.03, m	5
	69.0	4.01 m	5	68.5	4.09, m	5
8	36.8	1.66 m	6, 7, 9, 10	36.80	1.66, m	7, 9, 10
	36.9			36.85		
9	28.9	2.20, m	7, 8, 11	28.2	2.24, m	7, 8, 10, 11
				28.9		
10	132.3	5.62, dt (14.5, 7.1)	8, 9, 12	132.4	5.63, dt (14.4, 6.8)	8, 9, 12
	132.4			132.5		
11	131.06	6.06, dd (14.5, 10.4)	9, 13	131.09	6.06, dd (14.4, 10.4)	9, 13
	131.12			131.15		
12	131.9	6.11, dd (14.7, 10.4)	10, 11, 14	132.08	6.11, dd (14.3, 10.4)	10, 11, 14
	132.0			132.14		
13	134.2	5.48, dd (14.7, 8.3)	11, 14, 15, 25	134.1	5.47, dd (14.3, 8.7)	11, 14, 15, 25
	134.3			134.2		
14	40.9	2.30, m	25	41.2	2.34, m	12, 13, 15, 25
15	81.26	3.63, d (8.5)	13, 14, 16, 17,	81.3	3.69, d (8.1)	13, 14, 16, 17, 25,
	81.27		25, 26			26
16	138.4			138.0		
17	128.6	5.35, d (8.5)	15, 26, 27	127.6	5.31, d (9.3)	15, 18, 19, 26, 27
18	67.8	5.57, dq (8.5, 6.0)	16, 17, 19, 27	45.96	3.43, m	16, 17, 19, 27
				46.00		
19	173.7			212.7		
				212.8		
20	34.5	2.27, t (7.5)	19, 21, 22	40.8	2.44, m	19, 21, 22
				40.9		
21	27.2	1.59, tt (7.5, 7.5)	19, 20, 22, 23	26.1	1.52, m	19, 20, 22, 23
22	22.4	1.34, tq (7.5, 7.5)	20, 21, 23	22.6	1.28, tq (7.4, 7.4)	20, 21, 23
23	13.9	0.91, t (7.5)	20, 21, 22	14.1	0.90, t (7.4)	21, 22
24	5.9	1.67, s	3, 4, 5	5.9	1.66, s	3, 4, 5
					1.67, s	
25	17.2	0.86, d (6.5)	13, 14, 15	17.4	0.91, d (6.5)	13, 14, 15
26	11.6	1.69, s	15, 16, 17	12.0	1.680, s	15, 16, 17
				12.1	1.684, s	15, 16, 17
27	20.7	1.26, d (6.0)	17, 18	16.78	1.129, d (6.8)	17, 18
				16.82	1.133, d (6.8)	17, 18

[a]Recorded at 500 MHz. [b]Recorded at 125 MHz. [c]HMBC correlations are from proton(s) stated to the indicated carbon.

resolution ESITOFMS analysis gave the molecular formula $C_{27}H_{42}O_6$, which indicated a loss of one oxygen atom from **2**. The presence of an *n*-pentanoyl group was detected in the COSY spectrum, but the ester carbonyl carbon was missing in the ^{13}C NMR spectrum, and the methylene protons H20 and H21 of the *n*-pentanoyl group and H27 doublet methyl protons displayed HMBC correlations to a keto carbon at δ_C 212.8 (C19). This doublet methyl was correlated to a methine (δ_H 3.44; δ_C 46.1) that showed a COSY correlation to olefinic methine H17 and a long-range correlation to C19. These correlation data indicated that the ester oxygen in **2** was missing in **3**, where the *n*-pentanoyl group was directly connected to C14. Further NMR analysis confirmed that the remaining part from C1 to C15 was the same as the corresponding part of **2** (Figure 7, Table 1). Thus, the planar structure of **3** was determined as shown in Figure 5. The carbon skeleton of **3** was identical with that of the structure

DOI: 10.1021/acs.jnatprod.8b00071
J. Nat. Prod. XXXX, XXX, XXX−XXX

Table 2. Annotated Putative ORFs in the Biosynthetic Gene Cluster of Linfuranones

				protein homologue whose function is characterized	
orf6-	accession number	size (aa)	proposed function	description, origin, accession number	%[a]
134	WP_055480424	3083	PKS	type I polyketide synthase (cmiP4), *Streptomyces* sp. MJ635-86F5, BAO66529	53/64
133	WP_055480423	4795	PKS	modular polyketide synthase (Nmd1), *Streptomyces* sp. RK95-74, BAW35608	50/61
132	WP_055480220	3527	PKS	modular polyketide synthase (Nmd6), *Streptomyces* sp. RK95-74, BAW35613	56/66
131	WP_055480219	5362	PKS	type I modular polyketide synthase (PkeAIII), *Saccharopolyspora erythraea* NRRL 2338, AAQ94248	56/66
130	WP_055480218	1510	PKS	type I PKS (HcaA), *Streptomyces hygroscopicus*, CCF23200	51/60
129	WP_063842922	488	FAD-dependent monooxygenase	Baeyer–Villiger monooxygenase (ORF 8), *Streptomyces aculeolatus* NRRL 18422, ABB88524	52/66
128	WP_055480421	840	cytochrome P450 hydroxylase	monooxygenase AufB, *Stigmastella aurantiaca* DW4/3–1, CAO98846	56/70
127	WP_055480217	250	type II thioesterase	type II thioesterase, *Streptomyces* sp. NBRC 110027, GAO07626	53/70
126	WP_055480216	545	FAD-dependent monooxygenase	phenylacetone monooxygenase (PamO), *Thermobifida fusca* YX, AAZ55526	57/69

[a]Identity/similarity.

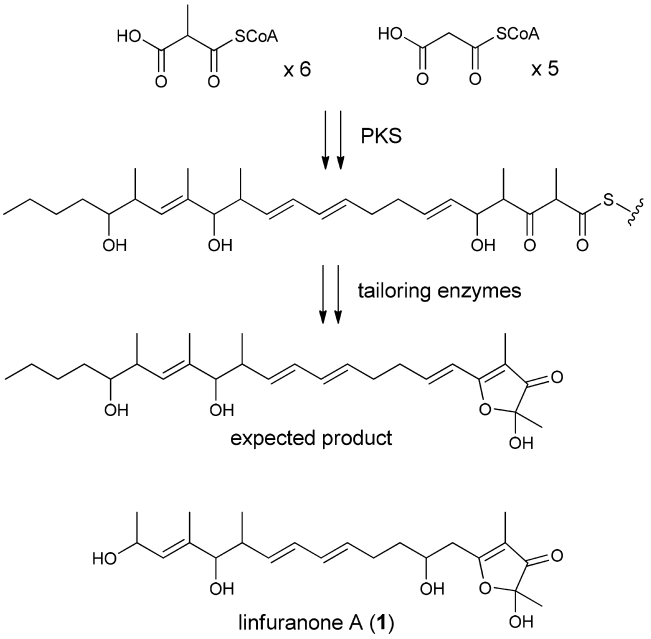

Figure 2. Structure of linfuranone skeleton predicted by *in silico* genomic analysis. See Figure 11 for biosynthetic gene organization.

predicted by *in silico* genomic analysis of the PKS gene cluster of linfuranones.

The absolute configurations at C7 and C15 were elucidated by chiral anisotropic analysis. Compound **3** was derivatized to MPA (α-methoxyphenylacetic acid) esters[6] by treatment with (*R*)- and (*S*)-MPA to give tris(*R*)- and (*S*)-MPA esters (**5a** and **5b**), respectively. The signs of $\Delta\delta_{R-S}$ values for the protons from H7 to H14 and H25 were positive, while those for H6, H14 to H18, and H25 to H27 were negative, establishing 7*R* and 15*R* configurations (Figure 8). Similar to the case of **2**, the relative configuration of the methyl group at C14 was assigned *anti* to the 15-OH group by NOESY analysis and a coupling constant.

The remaining chirality at C18 of **3** was determined through chemical degradation. In order to avoid epimerization at C18, the C19 keto group was reduced to a hydroxy group by L-selectride. Then, the C16–C17 double bond was cleaved by ozonolysis and following oxidative workup gave a mixture containing α-methyl-β-hydroxyheptanoic acid (*nat*-**6**) derived from the C17–C23 portion of **3** (Figure 9). This reaction mixture was subjected to (*R*)-PGME (phenylglycine methyl ester)[7] derivatization to obtain the corresponding amide, which was compared with the (*R*)-PGME amides of four possible synthetic stereoisomers of **6** by LC/MS (Figures 9 and 10). The (*R*)-PGME derivative prepared from degradation of **3** gave two peaks, corresponding to (2*S*,3*R*)- and (2*S*,3*S*)-**6** at 19.1 and 23.1 min, respectively, in a ratio of ca. 1:3. Therefore, the *S* configuration of the methyl group in **6** derived from **3** and thereby the 18*R* configuration for **3** were established.

Genome analysis of *S. mesophila* GMKU 363 identified three type I PKS gene clusters,[4] one of which was assigned to that for the linfuranone biosynthesis based on *in silico* analysis of PKS module/domain organizations (Figure 11). This type I PKS system comprises five open reading frames (*orf6–134*, *orf6–133*, *orf6–132*, *orf6–131*, *orf6–130*) encoding 11 modules. Module 1 was deduced as a loading module since the active site cysteine of the ketosynthase (KS) domain was replaced with glutamine.[8] Analysis of the signature amino-acid residues of AT domains predicted that AT domains in modules 1, 3, 4, 5, 10, and 11 have specificity to methylmalonyl-CoA and those

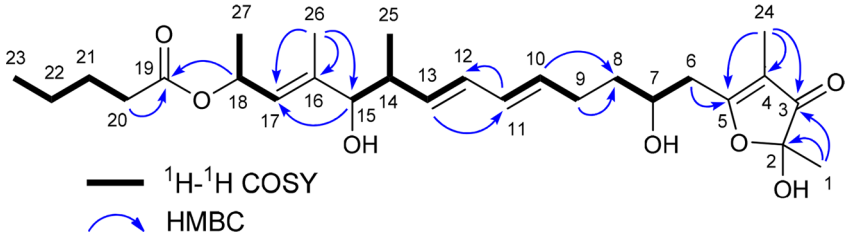

Figure 3. COSY and key HMBC correlations for linfuranone B (**2**).

DOI: 10.1021/acs.jnatprod.8b00071
J. Nat. Prod. XXXX, XXX, XXX–XXX

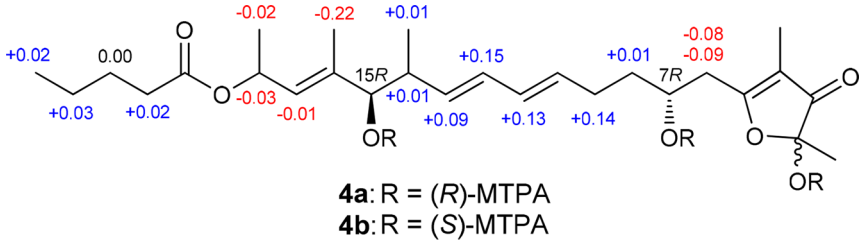

Figure 4. $\Delta\delta_{S-R}$ values for tris-MTPA derivatives (**4a** and **4b**) of **2**.

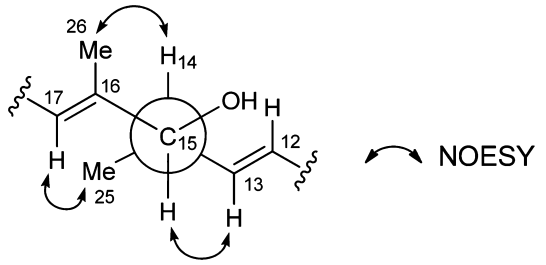

Figure 5. Relative configuration of C14 and C15 of **2** determined by NOEs.

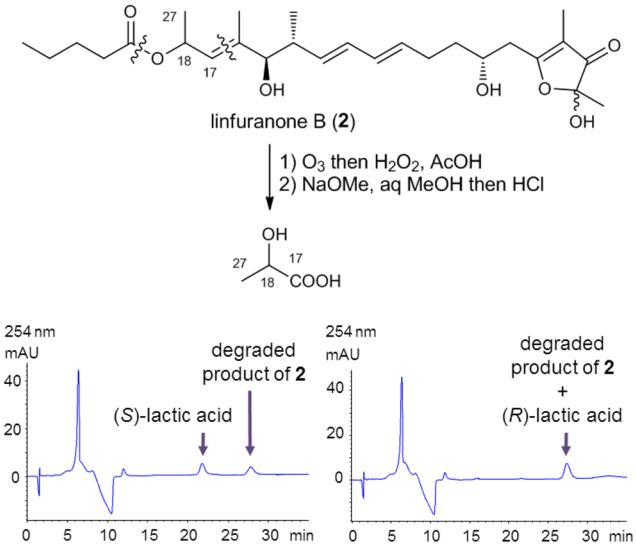

Figure 6. Chiral HPLC analysis of degraded product of **2**.

in modules 2, 6, 7, 8, and 9 likely incorporate the malonyl extender unit.[9] The structures of linfuranones suggested that the ketoreductase (KR) domain in module 3 and the dehydratase (DH) domain in module 9 are inactive, also being predicted by the sequence analysis that KR3 lacks active residues LDD and W,[10] and DH9 lacks hallmark motifs GYxYGPxF and LPFxW.[11] Three potential post-PKS tailoring enzymes are encoded in the linfuranone biosynthetic gene locus: two FAD-dependent monooxygenases (*orf6−129*, *orf6−126*) and a cytochrome P450 hydroxylase (*orf6−128*). The monooxygenase ORF6-129 has significant homology to Baeyer−Villiger monooxygenases ORF 8 (52% identity and 66% similarity), ORF 13 (48% identity and 58% similarity), and AufJ (47% identity and 61% similarity) responsible for furanone formation in the biosynthesis of E-837, E-492, and aurafurons, respectively.[2g,12] The hydroxylase ORF6-128 shows high homology to AufB (56% identity and 70% similarity) responsible for hydroxylation of the furanone unit in aurafuron biosynthesis.[12] ORF6-128 also displays high homology to the hydroxylases in the biosynthesis of E-837 and E-492.[2g] Another FAD-dependent monooxygenase, ORF6-126, shares high homology with phenylacetone monooxygease PamO from a thermophilic bacterium, *Thermobifida fusca* (57% identity and 69% similarity).[13] PamO has the ability to catalyze the Baeyer−Villiger oxidation of cyclic and acyclic ketones such as phenylacetone. Based on these *in silico* investigations, ORF6-126 is proposed to catalyze the oxygen insertion between C18 and C19 of linfuranone C (**3**) that gives rise to linfuranone B (**2**), whereas ORF6-129 and ORF6-128 are most likely involved in furanone formation (Figures 11 and 12). *Orf6-127* flanked by the oxidative tailoring enzymes in the biosynthetic gene cluster encodes a type II thioesterase (Table 2) which likely plays a roll of an editing enzyme that catalyzes the removal of aberrant polyketide intermediates inappropriately synthesized by PKSs.[14] As there is no hydrolytic enzyme encoded in or near the cluster, hydrolysis of **2** to **1** might be a nonenzymatic process.

As linfuranone A (**1**) has the ability to induce differentiation of murine ST-13 preadipocytes into mature adipocytes, effects of linfuranones B (**2**) and C (**3**) on the same cell lines were examined. By the treatment with 20 μM of **2** and **3**, 22% and 45% of preadipocytes were differentiated, respectively. Both compounds were more potent than **1** (9% differentiation at 20 μM). At the concentration of 40 μM, 33% and 73% of preadipocytes were differentiated into adipocytes by treatment with **2** and **3**, respectively. **2** and **3** were inactive against *Escherichia coli*, *Micrococcus luteus*, and *Candida albicans* at 25 μg/mL.

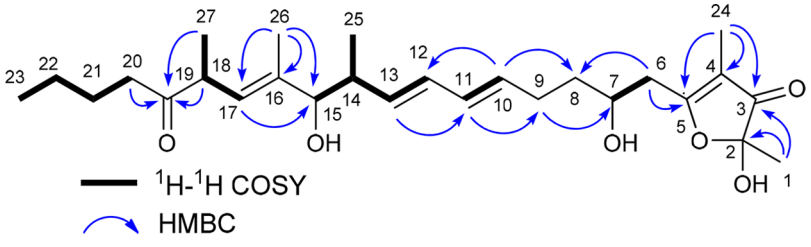

Figure 7. COSY and key HMBC correlations for linfuranone C (**3**).

DOI: 10.1021/acs.jnatprod.8b00071
J. Nat. Prod. XXXX, XXX, XXX−XXX

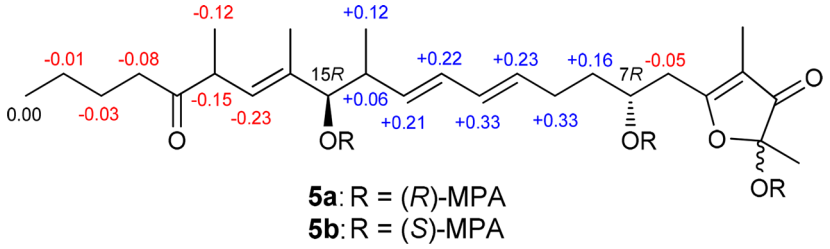

Figure 8. $\Delta\delta_{R-S}$ values for tris-MPA derivatives (**5a** and **5b**) of **3**.

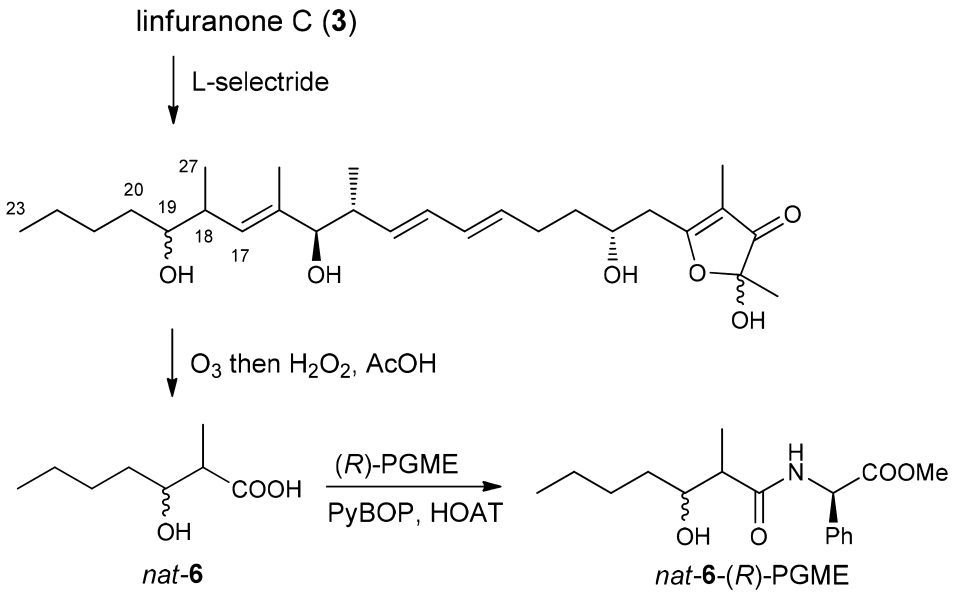

Figure 9. Degradation of **3** and PGME derivatization.

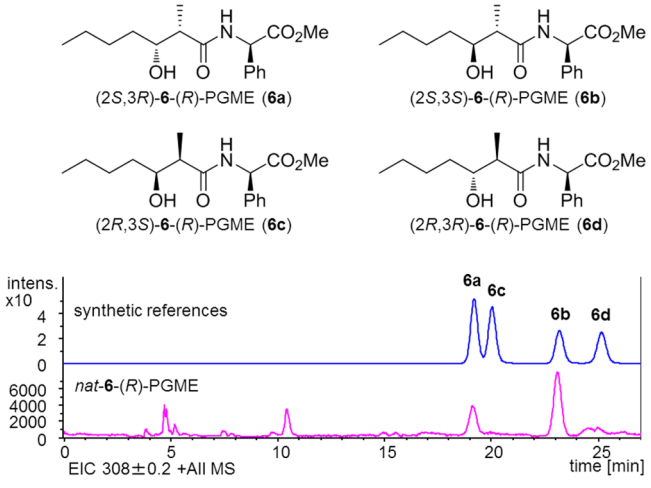

Figure 10. LC/MS analysis of the (*R*)-PGME derivative of the degraded product of **3**.

In conclusion, two new furanone-containing polyketides, linfuranones B (**2**) and C (**3**), were isolated from an actinomycete of the genus *Sphaerimonospora*. Compound **3** was discovered through *in silico* analysis of biosynthetic genes and temperature optimization for production fermentation. Compound **2** is generated from **3** by oxidative cleavage of the polyketide backbone by Baeyer−Villiger oxidation. This type of decoration of the polyketide main carbon chain is not common. DTX-4, a dinoflagellate metabolite, is a preceding example in which Baeyer−Villiger-type oxidation is involved in the oxygen insertion into a linear polyketide chain.[15]

EXPERIMENTAL SECTION

General Experimental Procedures. Optical rotations were measured using a JASCO DIP-3000 polarimeter. UV spectra were recorded on a Hitachi U-3210 spectrophotometer. IR spectra were measured on a PerkinElmer Spectrum 100. NMR spectra were obtained on a Bruker AVANCE 500 spectrometer in $CDCl_3$ using the signals of the residual solvent protons (δ_H 7.27) and carbons (δ_C 77.0) as internal standards. HR-ESITOFMS were recorded on a Bruker micrOTOF focus.

Microorganism. Strain GMKU 363 was isolated from a root of the Thai medicinal plant "Lin Ngu Hao" (*Clinacanthus siamensis* Bremek.) collected in Chachoengsao Province, Thailand. It was initially identified as a member of the genus *Microbispora* in our previous study.[3] However, this strain was reassigned to *Sphaerimonospora mesophila*[16] on the basis of genome sequence-based classification[17] in comparison with *Sphaerimonospora mesophila* NBRC 14179^T (BCRI00000000.1).

Fermentation. Strain GMKU 363 cultured on a Bn-2 agar medium consisting of 0.5% soluble starch, 0.5% glucose, 0.1% meat extract (Kyokuto Pharmaceutical Industrial Co., Ltd.), 0.1% yeast extract (Difco Laboratories), 0.2% NZ-case (Wako Pure Chemical Industries, Ltd.), 0.2% NaCl, 0.1% $CaCO_3$, and 1.5% agar was inoculated into 500 mL K-1 flasks each containing 100 mL of the V-22 seed medium (pH 7.0) consisting of 1% soluble starch, 0.5% glucose, 0.3% NZ-case, 0.2% yeast extract, 0.5% Tryptone (Difco Laboratories), 0.1% K_2HPO_4, 0.05% $MgSO_4 \cdot 7H_2O$, and 0.3% $CaCO_3$. The flasks were placed on a rotary shaker (200 rpm) at 37 °C for 4 days. The seed culture (5−10%) was transferred into 500 mL K-1 flasks each containing 100 mL of the A-11 M production medium

DOI: 10.1021/acs.jnatprod.8b00071
J. Nat. Prod. XXXX, XXX, XXX−XXX

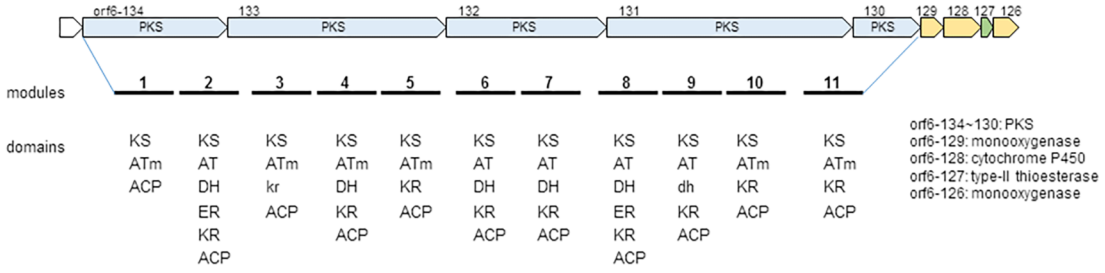

Figure 11. Putative biosynthetic gene cluster of linfuranones.

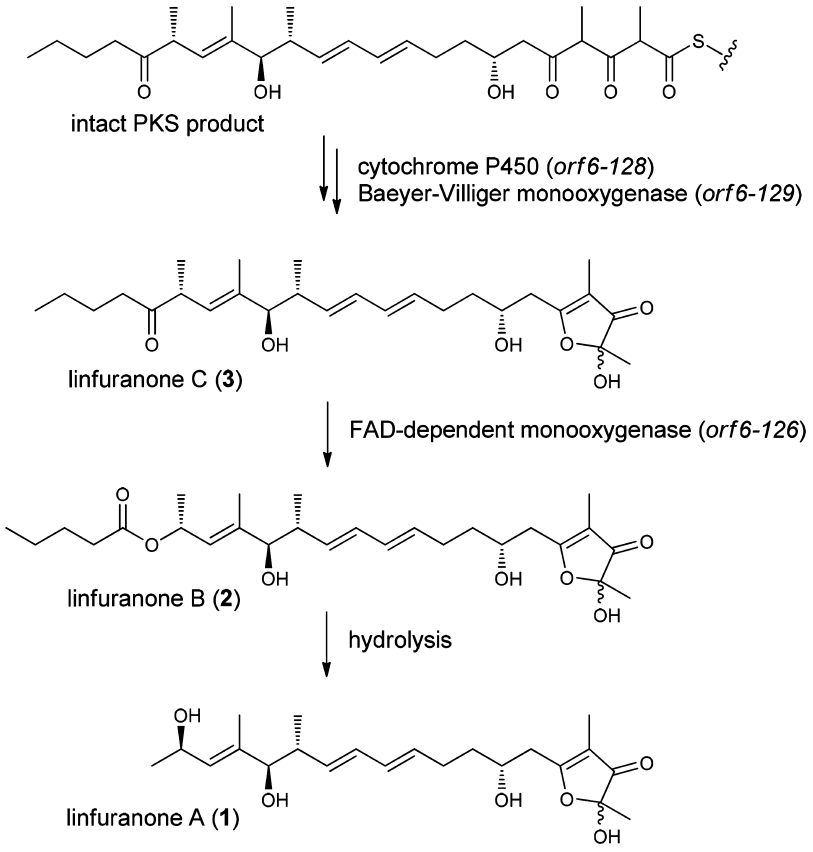

Figure 12. Plausible biosynthetic relationship among linfuranones A−C.

(pH 7.0) consisting of 2.5% soluble starch, 0.2% glucose, 0.5% yeast extract, 0.5% polypeptone (Wako Pure Chemical Industries, Ltd.), 0.5% NZ-amine (Wako Pure Chemical Industries, Ltd.), 0.3% $CaCO_3$, and 1% Diaion HP-20 (Mitsubishi Chemical Co.). The inoculated flasks were placed on a rotary shaker (200 rpm) at 37 °C for 7 days.

Extraction and Isolation. At the end of the fermentation period, 50 mL of 1-butanol was added to each flask, and the flasks were allowed to shake for 1 h. The mixture was centrifuged at 6000 rpm for 10 min, and the organic layer was separated from the aqueous layer containing the mycelium. Evaporation of the solvent gave approximately 7.8 g of crude extract from 10 L of culture. The crude extract (7.8 g) was subjected to silica gel column chromatography with a step gradient of $CHCl_3$−MeOH (1:0, 20:1, 10:1, 4:1, 2:1, 1:1, and 0:1 v/v). Fraction 4 (4:1) was concentrated to provide 2.2 g of brown oil, which was further purified by reversed-phase ODS column chromatography with a gradient of MeCN−H_2O (2:8, 3:7, 4:6, 5:5, 6:4, 7:3, and 8:2 v/v). Fraction 5 (6:4) was evaporated, and the remaining aqueous solution was extracted with EtOAc. After drying with anhydrous Na_2SO_4, the organic layer was concentrated to give semipure linfuranones. Final purification was achieved by preparative ODS (Cosmosil C_{18}-AR-II, 10 × 250 mm, Nacalai Tesque) HPLC using an isocratic MeCN/H_2O (50:50) at 4 mL/min, yielding linfuranone B (**2**, 141 mg, t_R 20.3 min) and linfuranone C (**3**, 22 mg, t_R 15.6 min) as a pale yellow, amorphous solid.

*Linfuranone B (**2**):* pale yellow, amorphous solid; $[\alpha]^{22}_D$ +77 (*c* 1.0, MeOH); UV (MeCN) λ_{max} (log ε) 232 (5.55), 282 (5.04); IR ν_{max} 3383, 1695, 1611 cm^{-1}; ^1H and ^{13}C NMR data, see Table 1; HRESITOFMS $[M - H]^-$ 477.2859 (calcd for $C_{27}H_{41}O_7$, 477.2858).

*Linfuranone C (**3**):* pale yellow, amorphous solid; $[\alpha]^{22}_D$ −67 (*c* 0. 40, MeOH); UV (MeCN) λ_{max} (log ε) 227 (4.86), 281 (4.87); IR ν_{max} 3383, 1695, 1611 cm^{-1}; ^1H and ^{13}C NMR data, see Table 1; HRESITOFMS $[M - H]^-$ 461.2905 (calcd for $C_{27}H_{41}O_6$, 461.2909).

*Tris(R)-MTPA ester of **2** (**4a**).* To a solution of **2** (2.0 mg, 4.2 μmol) in dry pyridine (100 μL) was added (*S*)-MTPA chloride (7 μL, 37 μmol) at room temperature. After standing for 1 h, the reaction mixture was concentrated under reduced pressure, and the residue was purified by silica gel column chromatography (*n*-hexane/EtOAc, 8:1−1:1) to give tris(*R*)-MTPA ester **4a** (2.8 mg, 60% yield): ^1H NMR (500 MHz, $CDCl_3$) δ 0.88 (H25), 0.89 (H23), 1.27 (H27), 1.32 (H22), 1.48 (H1), 1.50 (H1), 1.57 (H21), 1.73 (H26), 1.74 (H24), 1.75 (H24), 1.77 (H8), 1.99 (H9), 2.26 (H20), 2.50 (H14), 2.79 (H6), 3.01 (H6), 5.35 (H13), 5.51 (H17), 5.58 (H18), 5.81

DOI: 10.1021/acs.jnatprod.8b00071
J. Nat. Prod. XXXX, XXX, XXX−XXX

(H11), 5.87 (H12); HR-ESITOFMS *m/z* 1165.3756 $[M + K]^+$ (calcd for $C_{57}H_{63}F_9O_{13}K$ 1165.3757).

*Tris(S)-MTPA ester of **2** (**4b**).* In the same manner as described for **4a**, **4b** (2.7 mg, 55% yield) was prepared from **2** (2.0 mg) and (*R*)-MTPA chloride: ^{1}H NMR (500 MHz, $CDCl_3$) δ 0.89 (H25), 0.91 (H23), 1.25 (H27), 1.35 (H22), 1.51 (H26), 1.57 (H21), 1.61 (H1), 1.68 (H1), 1.78 (H8), 1.83 (H24), 1.84 (H24), 2.13 (H9), 2.28 (H20), 2.55 (H14), 2.71 (H6), 2.92 (H6), 5.44 (H13), 5.50 (H17), 5.55 (H18), 5.95 (H11), 6.02 (H12); HR-ESITOFMS *m/z* 1149.4010 $[M + Na]^+$ (calcd for $C_{57}H_{63}F_9O_{13}Na$ 1149.4017).

*Alkaline hydrolysis of **2** to linfuranone A (**1**).* Compound **2** (5.0 mg, 10 μmol) was dissolved in 5% NaOMe/MeOH (2.6 mL) and stirred for 30 min at room temperature. The reaction mixture was neutralized by adding 5% HCO_2H solution (4 mL) and then evaporated to dryness. The crude material was purified by HPLC using a Cosmosil C_{18}-AR-II column (10 × 250 mm) with an isocratic solvent system of 30% MeCN in distilled water at a flow rate of 4.0 mL/min, monitoring at 280 nm to yield **1** (2.3 mg, t_R = 12.1 min): $[\alpha]^{23}_D$ −3.0 (*c* 0.10, MeOH); ^{1}H and ^{13}C NMR data matched those of naturally occurring linfuranone A (**1**); HR-ESITOFMS *m/z* 393.2285 $[M - H]^-$ (calcd for $C_{22}H_{33}O_6$ 393.2283).

Oxidative Degradation of 2 and Chiral HPLC Analysis. To a solution of **2** (2.0 mg, 4.2 μmol) in EtOAc (5 mL) was bubbled O_3 at −78 °C until the solution turned pale blue. After bubbling oxygen into the solution at the same temperature for 15 min, HCO_2H (0.75 mL) and 30% H_2O_2 (0.44 mL) were added, and the reaction mixture was heated at 60 °C for 15 h. Then, the reaction mixture was evaporated under vacuum, the resultant material was dissolved in MeOH (200 μL), and 28% NaOMe solution (150 μL) was added. After standing for 18 h at ambient temperature, the reaction mixture was analyzed on a chiral HPLC (Sumichiral OA-5000, 4.6 × 150 mm; 1 mM $CuSO_4$ solution; 1.0 mL/min; detection at 254 nm). Retention times of the standard samples were 21.8 min for (*S*)-lactic acid and 27.8 min for (*R*)-lactic acid. Co-injection of the degraded product of **2** gave two peaks when injected with (*S*)-lactic acid and a single peak when injected with (*R*)-lactic acid.

*Tris(R)-MPA ester of **3** (**5a**).* To a solution of **3** (1.0 mg, 2.2 μmol) in dry CH_2Cl_2 (120 μL) were added (*R*)-MPA (1.5 mg, 9.0 μmol), *N*,*N*-dimethyl-4-aminopyridine (DMAP, trace amount), and a solution of diisopropylcarbodiimide (DIC, 1 mg, 7.9 μmol) in dry CH_2Cl_2 (20 μL) at room temperature. After standing for 30 min, the reaction mixture was diluted with ice/water and extracted with EtOAc. The organic layer was concentrated under reduced pressure, and the residue was purified by HPLC (*n*-hexane/EtOAc, 8:1−1:1) to give tris(*R*)-MPA ester **5a** (0.6 mg, 30% yield): ^{1}H NMR (500 MHz, $CDCl_3$) δ 0.88 (H23), 0.90 (H25), 0.93 (H27), 1.22 (H22), 1.43 (H21), 1.70 (H8), 1.98 (H9), 2.22 (H20), 2.49 (H14), 2.72 (H6), 3.16 (H18), 5.06 (H17), 5.40 (H13), 5.47 (H10), 5.85 (H11), 5.96 (H12); HR-ESITOFMS *m/z* 929.4445 $[M + Na]^+$ (calcd for $C_{54}H_{66}O_{12}Na$ 929.4446).

*Tris(S)-MPA ester of **3** (**5b**).* In the same manner as described for **5a**, **5b** (0.5 mg, 25% yield) was prepared from **3** (1.0 mg, 2.2 μmol) and (*S*)-MPA: ^{1}H NMR (500 MHz, $CDCl_3$) δ 0.78 (H25), 0.88 (H23), 1.05 (H27), 1.23 (H22), 1.46 (H21), 1.54 (H8), 1.66 (H9), 2.29 (H20), 2.44 (H14), 2.76 (H6), 3.31 (H18), 5.19 (H13), 5.23 (H10), 5.29 (H17), 5.52 (H11), 5.74 (H12); HR-ESITOFMS *m/z* 929.4447 $[M + Na]^+$ (calcd for $C_{54}H_{66}O_{12}Na$ 929.4446).

*Degradation of **3**.* To a stirred solution of **3** (0.25 mg, 0.5 μmol) in dry THF (50 μL) was added L-selectride (1.0 M THF solution, 10 μL, 0.5 μmol) at 0−5 °C. After 1 h, L-selectride (40 μL, 0.5 μmol) was further added to the solution, which was then stirred for 18 h at ambient temperature. The reaction was quenched with a saturated NH_4Cl solution and extracted with EtOAc. The organic layer was dried over anhydrous Na_2SO_4 and concentrated under reduced pressure. The residual material was dissolved in EtOAc (5 mL), to which was bubbled O_3 at −78 °C for 30 min. Then, formic acid (0.75 mL) and 30% H_2O_2 solution (0.40 mL) were successively added to the reaction mixture, and the temperature was gradually raised to 60 °C. After stirring for 15 h at the same temperature, the mixture was evaporated to dryness under reduced pressure. The residue was subjected to (*R*)-PGME amidation and the following LC/MS analysis.

*LC/MS analysis of the degradation product of **3**.* The (*R*)-PGME derivative of 3-hydroxy-2-methylheptanoic acid (**6**) derived from the degradation of **3** was compared with the (*R*)-PGME derivatives of four possible stereoisomers of **6** prepared by chemical synthesis (see Supporting Information). LC/MS analysis was performed on an Agilent HP1200 system and Bruker micrOTOF Focus using an ODS column (COSMOSIL 5C_{18}-AR-II, 2.0 × 150 mm) at a flow rate of 0.3 mL/min with an isocratic elution (40% MeCN in distilled water). Retention times of the standard samples were 19.3 min for (2*S*,3*R*)-**6**, 20.0 min for (2*R*,3*S*)-**6**, 23.1 min for (2*S*,3*S*)-**6**, and 25.1 min for (2*R*,3*R*)-**6**. Under the same conditions, the (*R*)-PGME derivative of the degraded product of **3** gave two peaks, at 19.1 and 23.1 min, corresponding to (2*S*,3*R*)- and (2*S*,3*S*)-isomers, respectively.

Adipocyte Differentiation Assay. The assay was carried out according to the reported procedure.[18] In brief, mouse-derived ST-13 preadipocytes were plated at 1 × 10^4 cells/mL in 24-well dishes containing 1 mL of a basal medium containing DME/F-12, 10% fetal bovine serum, 100 units/mL penicillin, and 100 μg/mL streptomycin on day 1 and cultured at 37 °C in a humidified atmosphere containing 5% CO_2. Moreover, the fresh basal medium containing the indicated concentrations of linfuranones (or 20 nM rosiglitazone (positive control)) was replaced on day 2, 5, and 8. On day 12, the ST-13 cells were washed three times with phosphate-buffered saline, fixed with 10% formalin neutral buffer solution at room temperature for 10 min, and then washed with distilled water to remove formalin solution. Furthermore, the cells were rinsed with 60% 2-propanol for 5 min, stained with 0.24% Oil Red O at room temperature for 20 min, and then photographed under a phase contrast microscope (100× magnification) equipped a CCD camera (Leica Microsystems Japan, Tokyo, Japan).

■ ASSOCIATED CONTENT

Supporting Information

The Supporting Information is available free of charge on the ACS Publications website at DOI: 10.1021/acs.jnatprod.8b00071.

Experimental procedures and 1D and 2D NMR spectra of compounds **2** and **3** (PDF)

■ AUTHOR INFORMATION

Corresponding Author

*Tel: +81-766-56-7500. Fax: +81-766-56-2498. E-mail: yas@pu-toyama.ac.jp.

ORCID

Yasuhiro Igarashi: 0000-0001-5114-1389

Notes

The authors declare no competing financial interest.

■ ACKNOWLEDGMENTS

This work was supported by JSPS KAKENHI Grant Number 24580156 to Y.I., Core-to Core Program, JSPS, and National Research Council of Thailand (NRCT) to A.T.

■ REFERENCES

(1) (a) Van Lanen, S. G.; Shen, B. *Curr. Opin. Drug Dev.* **2008**, *11*, 186−195. (b) Chen, H.; Du, L. *Appl. Microbiol. Biotechnol.* **2016**, *100*, 541−557.

(2) (a) Capon, R. J.; Faukner, D. J. *J. Org. Chem.* **1984**, *49*, 2506−2508. (b) Cimino, G.; Sodano, G.; Spinella, A. *J. Org. Chem.* **1987**, *52*, 5326−5331. (c) Kuroda, K.; Yoshida, M.; Uosaki, Y.; Ando, K.; Kawamoto, I.; Oichi, E.; Onuma, H.; Yamada, K.; Matsuda, Y. *J. Antibiot.* **1993**, *46*, 1196−1202. (d) Paul, M. C.; Zubia, E.; Ortega, M. J.; Salvia, J. *Tetrahedron* **1997**, *53*, 2303−2308. (e) Kunze, B.;

DOI: 10.1021/acs.jnatprod.8b00071
J. Nat. Prod. XXXX, XXX, XXX−XXX

Reichenbach, H.; Mueller, R.; Hoefle, G. *J. Antibiot.* **2005**, *58*, 244−251. (f) Cho, J. Y.; Kwon, H. C.; Williams, P. G.; Kauffman, C. A.; Jensen, P. R.; Fenical, W. *J. Nat. Prod.* **2006**, *69*, 425−428. (g) Banskota, A. H.; McAlpine, J. B.; Sørensen, D.; Aouidate, M.; Piraee, M.; Alarco, A.-M.; Ōmura, S.; Shiomi, K.; Farnet, C. M.; Zazapoulos, E. *J. Antibiot.* **2006**, *59*, 168−176. (h) Bromley, C. L.; Popplewell, W. L.; Pinchuck, S. C.; Hodgson, A. N.; Davies-Coleman, M. T. *J. Nat. Prod.* **2012**, *75*, 497−501. (i) Okanya, P. W.; Mohr, K. I.; Gerth, K.; Kessler, W.; Jansen, R.; Stadler, M.; Müller, R. *J. Nat. Prod.* **2014**, *77*, 1420−1429. (j) Fujiwara, K.; Tsukamoto, H.; Izumikawa, M.; Hosoya, T.; Kagaya, N.; Takagi, M.; Yamamura, H.; Hayakawa, M.; Shin-ya, K.; Doi, T. *J. Org. Chem.* **2015**, *80*, 114−132.

(3) Indananda, C.; Igarashi, Y.; Ikeda, M.; Oikawa, T.; Thamchaipenet, A. *J. Antibiot.* **2013**, *66*, 675−677.

(4) Komaki, H.; Ichikawa, N.; Hosoyama, A.; Fujita, N.; Thamchaipenet, A.; Igarashi, Y. *Genome Announc.* **2015**, *3*, e01471−15.

(5) Ohtani, I.; Kusumi, T.; Kashman, Y.; Kakisawa, H. *J. Am. Chem. Soc.* **1991**, *113*, 4092−4096.

(6) Trost, B. M.; Belletire, J. L.; Godleski, S.; McDougal, P. G.; Balkovec, J. M.; Baldwin, J. J.; Christy, M. E.; Ponticello, G. S.; Varga, S. L.; Springer, J. P. *J. Org. Chem.* **1986**, *51*, 2370−2374.

(7) Yabuuchi, T.; Kusumi, T. *J. Org. Chem.* **2000**, *65*, 397−404.

(8) Bisang, C.; Long, P. F.; Cortés, J.; Westcott, J.; Crosby, J.; Matharu, A. L.; Cox, R. J.; Simpson, T. J.; Staunton, J.; Leadlay, P. F. *Nature* **1999**, *401*, 502−505.

(9) Kakavas, S. J.; Katz, L.; Stassi, D. *J. Bacteriol.* **1997**, *179*, 7515−7522.

(10) Keatinge-Clay, A. T. *Chem. Biol.* **2007**, *14*, 898−908.

(11) Keatinge-Clay, A. *J. Mol. Biol.* **2008**, *384*, 941−953.

(12) Frank, B.; Wenzel, S. C.; Bode, H. B.; Shcarfe, M.; Blöcker, H.; Müller, R. *J. Mol. Biol.* **2007**, *374*, 24−38.

(13) (a) Dudek, H. M.; Torres Pazmiño, D. E.; Rodriquez, C.; de Gonzalo, G.; Gotor, V.; Fraaije, M. W. *Appl. Microbiol. Biotechnol.* **2010**, *88*, 1135−1143. (b) Dudek, H. M.; et al. *Appl. Environ. Microbiol.* **2011**, *77*, 5730−5738.

(14) Wright, J. L. C.; Hu, T.; McLachlan, J. L.; Needham, J.; Walter, J. A. *J. Am. Chem. Soc.* **1996**, *118*, 8757−8758.

(15) Kotowska, M.; Pawlik, K. *Appl. Microbiol. Biotechnol.* **2014**, *98*, 7735−7746.

(16) Mingma, R.; et al. *Int. J. Syst. Evol. Microbiol.* **2016**, *66*, 1735−1744.

(17) Meier-Kolthoff, J. P.; Auch, A. F.; Klenk, H. P.; Göker, M. *BMC Bioinf.* **2013**, *14*, 60.

(18) (a) Kunimasa, K.; Kuranuki, S.; Matsuura, N.; Iwasaki, N.; Ikeda, M.; Ito, A.; Sashida, Y.; Mimaki, Y.; Yano, M.; Sato, M.; Igarashi, Y.; Oikawa, T. *Bioorg. Med. Chem. Lett.* **2009**, *19*, 2062−2064. (b) Ikeda, M.; Kurotobi, Y.; Namikawa, A.; Kuranuki, S.; Matsuura, N.; Sato, M.; Igarashi, Y.; Nakamura, T.; Oikawa, T. *Med. Chem.* **2011**, *7*, 250−256.

DOI: 10.1021/acs.jnatprod.8b00071
J. Nat. Prod. XXXX, XXX, XXX−XXX